Zhou *et al. Acta Neuropathologica Communications* (2025) 13:56
https://doi.org/10.1186/s40478-025-01967-4

Acta Neuropathologica Communications

RESEARCH Open Access

Targeting NAD + biosynthesis suppresses TGF-β1/Smads/RAB26 axis and potentiates cisplatin cytotoxicity in non-small cell lung cancer brain metastasis

Liyun Zhou[1†], Zhiying Li[2†], Shengli Zhou[3†], Bin Wang[1], Zhen Liang[4], Sen Hu[1], Hang Zhang[1], Lin Duan[1], Dongxu Zhao[1], Luyao Cheng[1], Hang Ren[1], Hiroaki Wakimoto[5*] and Ming Li[1*]

Abstract

Nicotinamide adenine dinucleotide (NAD^+) plays an important role in tumor progression, but its role in non-small cell lung cancer with brain metastasis (NSCLC BM) remains unclear. Herein, we investigated NAD^+ biosynthesis targeting as a new therapeutic strategy for NSCLC BM. Therapeutic activity of nicotinamide phosphoribosyl transferase (NAMPT) inhibitors was evaluated in mouse models of NSCLC BM and using various assays such as NAD^+ quantitation, cell viability, and apoptosis assays. To explore impact on downstream signaling, RNA sequencing was used in NAMPT inhibitor-treated and control cells, followed by validation with genetic knockdown, western blot and qRT-PCR. Expression of NAMPT and downstream proteins in human NSCLC BM and its association with patient prognosis were examined. Finally, combination of NAMPT inhibitor and cisplatin was tested in vivo. Systemic treatment with NAMPT inhibitors demonstrated intracranial activity in an NSCLC BM model. NAMPT inhibitors decreased cellular NAD levels and suppressed proliferation and invasion, and induced apoptosis in NSCLC cells. Supplementation with NAD^+ precursor NMN rescued these NAMPT inhibitor effects. Mechanistically, disruption of NAMPT-mediated NAD^+ biosynthesis suppressed TGF-β1/Smads/RAB26 signaling, leading to inhibition of NSCLC cells. Expression of NAMPT/TGF-β1/Smads/RAB26 axis proteins was upregulated in NSCLC BM tissues and correlated with poor prognosis. Combining NAMPT inhibitors with cisplatin further extended the survival of NSCLC BM-bearing mice. Targeting NAD^+ biosynthesis provides a new therapeutic strategy for NSCLC BM and can be effectively combined with cisplatin. Our studies identified the TGF-β1/Smads/RAB26 signaling downstream of NAMPT, which was targeted by NAMPT inhibition to mediate anti-cancer effects.

Keywords Non-small cell lung cancer brain metastasis, Nicotinamide adenine dinucleotide, Cisplatin

†Liyun zhou, Zhiying Li and Shengli Zhou contributed equally to this article.

*Correspondence:
Hiroaki Wakimoto
HWAKIMOTO@mgh.harvard.edu
Ming Li
MINGLI@zzu.edu.cn

Full list of author information is available at the end of the article

Introduction

Lung cancer is a leading cause of cancer-related death worldwide [1, 2], and metastasis is the leading cause of the high mortality of lung cancer [3]. The brain is the predominant secondary metastasis site for lung cancer compared with other common epithelial malignancies [4]. Approximately 20–65% of non-small cell lung cancer (NSCLC) patients suffer from brain metastasis (BM) [4, 5]. Despite aggressive clinical management, surgical resection, whole brain radiation, systemic chemotherapy, and molecular targeted therapies et al., improving survival time for patients and the prognosis of NSCLC BM still pose remarkable challenges. Thus, it is pivotal to investigate more effective treatment options.

Nicotinamide adenine dinucleotide (NAD^+), an important mediator of energy metabolism and signal transduction pathways, serves as a substrate for numerous enzymes and plays an important role in maintaining body homeostasis [6–8]. Recent studies have found that NAD^+ metabolic imbalance is closely related to tumor development and metastasis [9]. Nicotinamide phosphoribosyltransferase (NAMPT), the rate-limiting enzyme in the salvage NAD^+ biosynthetic pathway, was upregulated in multiple tumors [10–12], and targeting NAD^+ metabolism has great potential for tumor therapy. We have shown that NAMPT inhibitors could crosses the blood brain barrier (BBB), modulate the microenvironment of glioblastoma (GBM) and upregulate the expression of PD-L1 level, significantly extending the survival of GBM bearing animals [13, 14]. Moreover, BRAF inhibitor resistant (BiR) melanoma patients overexpress NAMPT, and NAMPT inhibitors could improve the survival of BiR xenografts [15]. However, the anticancer role of targeting NAD^+ metabolism in NSCLC BM remains unclear.

The present study aimed to address this knowledge gap. We showed that NSCLC BM tissues and NSCLC cells contained high level NAD^+, targeting NAD^+ inhibited intracranial tumor growth in NSCLC BM-bearing animals, and NAMPT inhibitor combined with cisplatin significantly prolonged the survival of animal models. Our study provides a mechanistic rationale to combine NAMPT inhibitor with cisplatin to yield durable responses in NSCLC BM.

Materials and methods

Cells

Mouse NSCLC cell line LLC, LLC cells with stable luciferase expression (LLC-luc), human NSCLC cell lines (H460, A549, H1975, H1922, PC9), immortalized human bronchial epithelial cell line (BEAS-2B), and mouse lung epithelial cell line (MLE-12) were used. The LLC and LLC-luc cells were purchased from the National Platform for Experimental Cell Resources (Beijing, China). H460 and A549 cell were purchased from the ATCC. H1975, H1922 and PC9 were kindly provided by the laboratory of Xiaojv Zhang (Respiratory and critical Care Center, Zhengzhou, China). BEAS-2B and MLE-12 cells were purchased from Zhongqiaoxinzhou Biotech (Shanghai, China).

All human cells were cultured in RPMI 1640 medium (VivaCell, Shanghai, China), with 10% fetal bovine serum (FBS) (Viva Cell, Shanghai, China), 100 U/ml penicillin G, and 100 μg/mL streptomycin at 37 °C with 5% CO_2, except the LLC and BEAS-2B cells, which were cultured in Dulbecco's Modified Eagle Medium (DMEM) (Viva Cell, Shanghai, China) with 10% FBS, 100 U/ml penicillin G, and 100 μg/mL streptomycin.

Animal study

Animal study was approved by the 7th People's Hospital of Zhengzhou Animal Care and Use Committee. Experimental procedures were performed in accordance with the Guide for the Care and Use of Laboratory Animals and according to the institutional ethical guidelines for animal experiments.

Male wild-type C57BL/6 mice (8–10 weeks, 25 ± 2 g) were purchased from Huaxing Animal Farm (Zhengzhou, China). All animals were housed with a temperature at 25 ± 1 ℃, SPF levels, pathogen-free and water and food were freely accessed.

Surgical procedures

Mice were implanted intracranially with 1×10^6 LLC-Luc cells in 5 μl PBS. On day 7, baseline bioluminescent imaging (BLI) was performed to observe the formation of intracranial tumors. For survival studies, the LLC-Luc-inoculated mice were treated with vehicle, FK866 5 mg/kg or FK866 10 mg/kg injected intraperitoneally twice every day on 4 days on/3 days off cycles until neurologic deficits or weight loss became significant. For immunohistochemistry analysis, LLC-Luc-inoculated mice were treated with vehicle, FK866 (5 mg/kg) or FK866 (10 mg/kg) injected intraperitoneally twice a day on the 4 days on/3 days off cycle that continued for 14 days, then euthanized 21 days after tumor implantation for preparing paraffin blocks of the brains.

For investigation of the effect of FK866 combined with cisplatin on the survival of animal models with NSCLC BM, mice were implanted intracranially with 1×10^6 LLC-Luc cells in 5 μl PBS. On day 7, mice were treated with vehicle or FK866 (10 mg/kg, twice per day, 4 days on/3 days off therapy) or cisplatin (4 mg/kg, once per week) or FK866 (10 mg/kg, twice per day 4 days on/3 days off therapy) + cisplatin (4 mg/kg, once per week) injected intraperitoneally until mice developed neurologic deficits or significant weight loss.

To analyze the effect of NAMPT inhibitors (FK866 and GMX1778) in the NSCLC model, mice were inoculated

subcutaneously in the flank with 1×10^5 LLC cells. On day 7, LLC-inoculated mice were randomly assigned into 3 groups and intratumorally treated with vehicle, FK866 (10 mg/kg, twice a day for 4 days on/3 days off therapy) or GMX1778 (50 mg/kg, once a day). On day 14, the subcutaneous tumors were removed and weighed.

Baseline BLI took place between 10 and 28 days after tumor cells implantation. The mice were injected intraperitoneally with luciferin (15 mg/ml, 10 μl/g) based on body weight, and anesthetized with 2% isoflurane. Images were acquired 10 min after luciferin injection.

Human samples

NSCLC and NSCLC BM samples were obtained from the People's Hospital of Zhengzhou university, Zhengzhou, China ($n = 10$, 6 males and 4 females, age 45 to 67 years old). All procedures were conducted with the approval of the Ethical Committee of the People's Hospital of Zhengzhou university and performed in accordance with relevant regulations and guidelines.

Immunohistochemistry (IHC) staining

For the IHC assay, tissue sections were prepared according to the established protocol [16]. The tissue sections were incubated overnight with primary antibodies at 4℃ and incubation with enhanced enzyme-labeled goat anti-mouse/rabbit IgG (PV-9000, ZSGB-BIO, China) was conducted at 37℃ for 60 min, followed by DAB staining and hematoxylin staining at room temperature for 5–60 s. The IHC staining intensity was analyzed using Image-Pro Plus 6.0 software (Media Cybernetics, Inc., Rockville, MD). The antibody information is listed in Table S1.

Cell counting Kit-8 assay

FK866 and GMX1778 were dissolved in Dimethyl sulfoxide (DMSO, Solarbio, China) at a stock concentration of 5 mM. β-Nicotinamide mononucleotide (NMN, MCE, USA)was reconstituted in ddH_2O at a stock concentration of 100 mM. Cells were plated at a density of 2,000 cells/well in 96-well plates, treated with vehicle, FK866, GMX1778, NMN for 48–72 h. Cell Counting Kit-8 (CCK-8, Meilunbio, Dalian, China) was subsequently added, and cells were further cultured for 1–4 h in a 37 °C incubator. The absorbance was detected at 450 nm (OD450) by a microplate reader (Potenov, China). The half maximal inhibitory concentration (IC50) values were generated and compared using GraphPad Prism.

EdU cell proliferation assay

The cell proliferation assay was performed using an EdU kit (BeyoClick™ EdU Cell Proliferation Kit with Alexa Fluor 555, Beyotime, China). Firstly, cells were seeded in 24-well plates and cultured with vehicle, FK866, GMX1778, or NMN for 48 h. Then, cells were incubated with EdU for 2 h, fixed with 4% paraformaldehyde at room temperature for 15 min, treated with 0.3% Triton X-100 for another 15 min, incubated with 1x Click reaction cocktail at room temperature for 30 min in a dark place, and stained with 1x Hoechst 33,342 at room temperature for 10 min in a dark place. After washing with 1 x PBS three times, images were taken.

Colony formation assay

To study the clonogenic potential, cells were plated at a density of 1,000 cells/well in 6-well plates and treated with vehicle, FK866, GMX1778, or NMN for 12 days (the media were replaced every 3 days). Then, cells were fixed with 4% paraformaldehyde at room temperature for 15 min and stained with 0.1% crystal violet at room temperature for 15 min in a dark place. After washing with 1 x PBS three times, colonies were counted.

NAD+ quantification

NAD^+ concentrations were measured using a NAD^+/NADH Assay Kit with WST-8 (Beyotime, China) according to the manufacturer's protocol. Absorbance values at OD450 were detected by the microplate reader.

Cell apoptosis and cycle assay

Cells were plated at a density of 10,000 cells/well in 6-well plates, and treated with vehicle, FK866, GMX1778, or NMN for 48 h. Then cells were centrifuged at 1,200 rpm for 5 min and resuspended in 100 μl 1x binding buffer. 5 μl Annexin V-FITC and 5 μl 7-ADD were added to stain cells for 15 min at room temperature in a dark place. Finally, 400 μl 1x binding buffer was added to samples and cell apoptosis was detected by flow cytometry (Becton Dickinson, US) and analyzed by Flow J software.

Cells were plated at a density of 1×10^5 cells/well in 6-well plates for 24 h, treated with vehicle, FK866, GMX1778, or NMN for 48 h. Cells were centrifuged at 800 rpm for 5 min and fixed with 70% alcohol at 4℃ for 8 h. To measure cell cycle, the samples were stained with 500 μl PI/RNase (Becton Dickinson, US) at room temperature for 15 min in a dark place, followed by flow cytometry to detect cell cycle distribution. The cell cycle was analyzed by Modfit software.

Wound healing assay

Cells were plated at a density of 1×10^5 cells/well in 6-well plates. Briefly, a pipette tip was used to create a scratch. Subsequently, FK866, GMX1778 and NMN were added to the FBS-medium and cultured for 48 h. Images were taken to measure cell migration under the microscope at 0 h, 24 h and 48 h, respectively. The scratch width was measured by Image J software.

Cell migration assay

A transwell chamber with 8-μm pore size membrane (Corning, USA) was used to determine the migration ability of cells in each group. Firstly, cells were plated at a density of 1×10^5 cells/well in 6-well plates, and treated with vehicle, FK866, GMX1778, or NMN for 48 h. Subsequently, 1×10^5 cells were suspended in 200 μl FBS-free medium and plated to the upper compartment, while 600 μl medium supplemented with 20% FBS was added to the lower compartment. After 24 h, cells were fixed with 4% paraformaldehyde at room temperature for 20 min and stained with 0.1% crystal violet at room temperature for 30 min in a dark place. Finally, cells that migrated into the lower compartment were counted under the microscope.

RNA sequencing (RNA-seq) and quantitative real-time PCR (qRT-PCR)

Total RNA was extracted from cells with TRIzol reagent (Invitrogen, USA). The second-generation RNA sequencing (RNA-seq) (BGI, China) was performed in accordance with the manufacturer's instructions. RESM (V1.2.8) software was used to calculate the gene expression of each group. DESeq was used for analysis of expressed genes between FK866-treated group and non-FK866-treated group; genes with a fold change ≥ 2 and adjusted P value ≤ 0.001 were defined as differentially expressed. PossionDIS was used for analysis of expressed genes between groups; genes with a fold change ≥ 2 and FDR ≤ 0.001 were defined as differentially expressed. For qRT-PCR analysis, cDNAs were synthesized using a reverse transcriptase kit (Transgen Biotech, China). Finally, the levels of RNA transcripts were quantified using quantitative kit (Transgen Biotech, China). To calculate relative gene expression, gene expression was normalized to β-actin and analyzed by the $2^{-\Delta\Delta Ct}$ method. qRT-PCR primers are shown in Table S2.

SiRNA

We purchased si-RAB26 silencing vector and corresponding negative control (si-NC) from Shenggong (China). si-RAB26 and si-NC were transfected into NSCLC cell lines (H460, A549) using lipofectamine 2000 kit (Thermo Fisher Scientific, USA). The target sequences of the siRNAs are shown in Table S3

Western blot

Total protein was isolated from cells using RIPA buffer (Solarbio, China) with 1% PMSF (Solarbio, China). Western blot was performed according to the manufacturer's protocol; protein bands were visualized with the ECL solution (Meilunbio, China). The protein bands gray value was analyzed by ImageLab software.

Statistical analysis

Each experiment was independently performed at least three times. All data were expressed as mean ± SD. The survival of the mice was analyzed using the Kaplan-Meier method, and log-rank test was used to compare survival time between two groups. SPSS 26.0 software and Graphpad Prism 5.0 software were used for all data analyses. $P < 0.05$ was considered statistically significant.

Results

FK866 inhibits tumor growth and prolongs survival in an NSCLC BM model

To determine whether FK866 inhibits NSCLC model growth and prolongs survival, mice intracranially implanted with LLC-Luc cells were treated with vehicle, FK866 (5 mg/kg or 10 mg/kg) twice per day on the 4 days on/3 days off cycles (Fig. 1A). FK866 suppressed tumor growth (Fig. 1B) and maintained body weight (Fig. 1C). In addition, FK866 treatment at both doses prolonged overall survival ($P < 0.01$)(Fig. 1D). IHC analysis of post-treatment tumors showed that Ki67 expression positivity was statistically significantly decreased in the FK866 groups (Fig. 1E-F).

In addition, we determined the antitumor activity of NAMPT inhibition (FK866, GMX1778) using a mouse subcutaneous NSCLC tumor model. The results showed that FK866 or GMX1778 injected intratumorally resulted in significant inhibition of tumor growth (Supplementary Fig. S1). These results indicate that NAMPT inhibition can inhibit the proliferation of NSCLC cells and tumor growth in vivo, intracranially and subcutaneously.

NAMPT inhibitors inhibit proliferation and colony formation of NSCLC cells

We investigated whether NAMPT inhibitors suppress the growth of NSCLC cells. Cell viability analysis showed that NSCLC cells were sensitive to NAMPT inhibitors at 48 h (Fig. 2A-B) and 72 h (Supplementary Fig. S2). NSCLC cells' viability was dramatically inhibited by NAMPT inhibitors. Consistent with the role of NAMPT in NAD^+ metabolism, the intracellular NAD^+ levels in NSCLC cells were significantly decreased with NAMPT inhibitors (Fig. 2C-D). Supplementation with NMN rescued cell viability (Fig. 2E) and NAD^+ levels (Fig. 2F).

EdU assay was performed to assess the changes in DNA synthesis in NSCLC cells treated with NAMPT inhibitors. A significant reduction for DNA synthesis was observed in NAMPT inhibitor-treated cells, compared with control cells (Supplementary Fig. S3A); supplementation with NMN rescued DNA synthesis (Supplementary Fig. S3B). Consistently, NAMPT inhibitors suppressed colony formation (Fig. S4A), and supplementation with NMN attenuated NAMPT inhibitor-induced

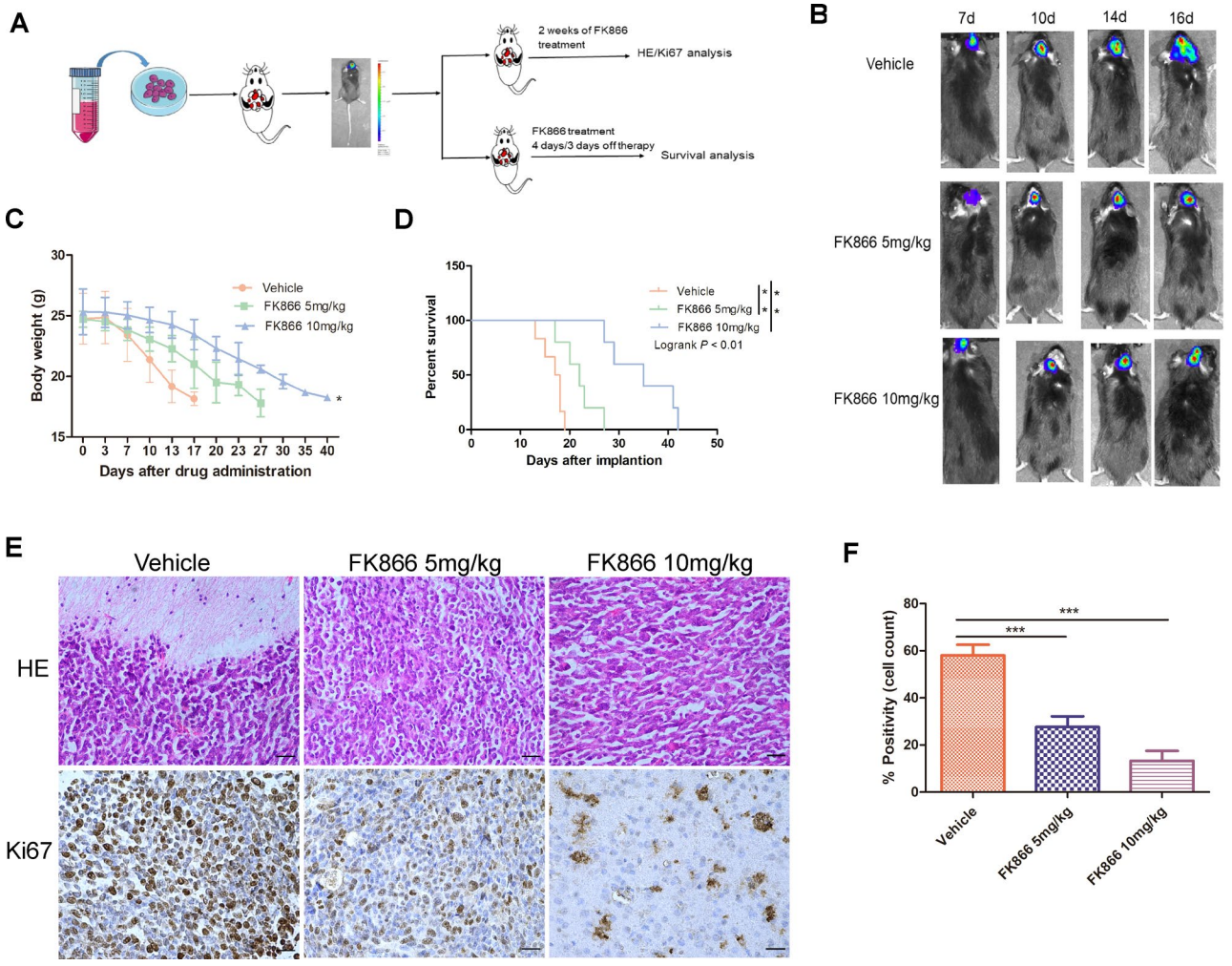

Fig. 1 FK866 inhibits NSCLC BM tumor growth and increases the survival of animals. **(A)** A mouse NSCLC line LLC was stably transfected with luciferase to allow for BLI. C57BL/6J mice ($n = 5–8$ mice per group) were injected intracranially with LLC-luc cells. 7 days after tumor implantation, LLC-luc-bearing mice were treated with FK866. **(B)** The set of LLC-luc-bearing mice were followed for BLI that occurred on days 7, 10, 14 and 16 while on treatment. **(C)** Animal weight was recorded for each group. **(D)** Survival data were collected for each group and analyzed by Kaplan–Meier analysis. **(E)** Representative microscopic images of Hematoxylin and Eosin staining and IHC for Ki-67 in intracranial LLC-luc tumors after 14-day treatment of mice. (*Scale bar*: 150 μm) **(F)** Quantification of percent positivity of Ki-67 IHC. *P<0.05, ** P < 0.01, *** P < 0.001

colony formation inhibition (Supplementary Fig. S4B and C).

NAMPT inhibitors induce apoptosis and arrest cell cycle at the S phase in NSCLC cells

To find out whether NAD^+ metabolism disruption is associated with cell apoptosis, we measured the percentage of apoptotic cells by flow cytometry, which showed that the percentage of NSCLC cells undergoing apoptosis increased in the groups of FK866 and GMX1778 treatment in a dose dependent manner ($P < 0.05$, one-way ANOVA) (Supplementary Fig. S5A). Consistently, Western blot showed that pro-apoptotic Bax was significantly increased and anti-apoptotic Bcl2 was significantly decreased in NAMPT inhibitors groups (Supplementary Fig. S5B and C).

To shed light on the interaction of NAD^+ metabolism and cell cycle progression, we exposed the cells to FK866 and performed cell cycle analysis of PI-stained ethanol-fixed cells. The proportion of cells in the S phase increased significantly, and the proportion of cells in the G1 phase decreased (Supplementary Fig. S5D). Western blot analysis of key cell cycle proteins showed that PCNA, CDK1, CDK2, and CyclinD1 levels were significantly decreased in NAMPT inhibitors groups in a dose dependent manner (Supplementary Fig. S5E and F). As expected, supplementation with NMN rescued Bcl2, CDK1, CDK2 levels (Supplementary Fig. S5G) and cells from apoptosis (Supplementary Fig. S6A and B). These results provide evidence for an interrelationship between NAD^+ metabolism, cell cycle, and cell apoptosis;

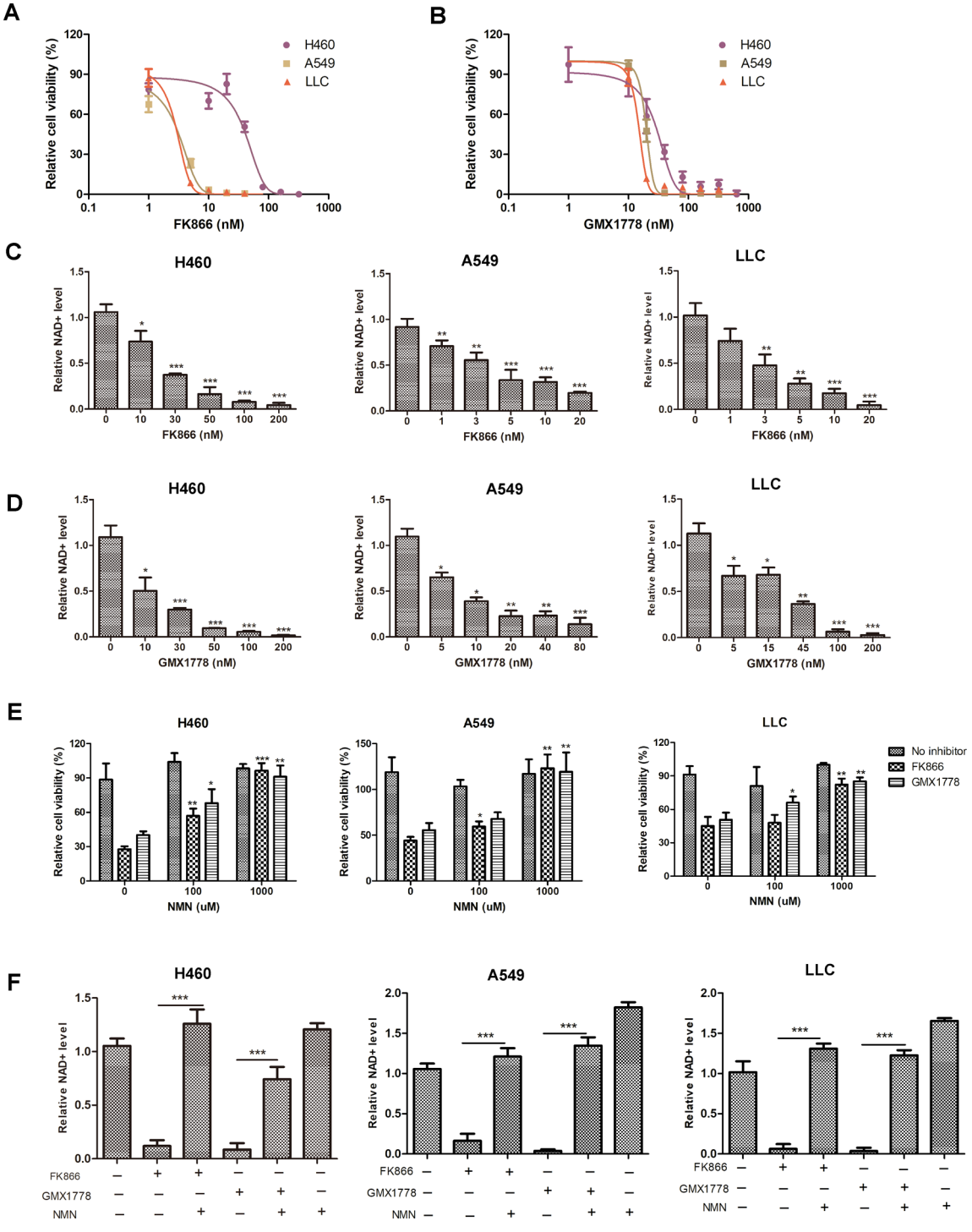

Fig. 2 NAMPT inhibitors deplete NAD + and inhibit NSCLC cell proliferation. H460, A549 and LLC cells were treated with 0.1%DMSO, FK866 and GMX1778 for 48 h, and **(A-B)** cell viability was measured by CCK-8 assay. **(C-D)** NAD^+ levels by NAD^+ quantification. **(E)** Impact of supplementation with NMN on cell viability by CCK8. **(F)** Impact of supplementation with NMN on NAD^+ levels by NAD^+ quantification. *P<0.05, ** P < 0.01, *** P < 0.001

NAMPT inhibitors arrest the cell cycle at the S phase and induce apoptosis in NSCLC cells.

NAMPT inhibitors inhibit migration of NSCLC cells

To investigate effects of NAD^+ metabolism on cell migration and invasion of NSCLC cells, wound-healing assays and transwell migration and invasion assays were used to assess the migratory and invasive activities of NSCLC cells. The wound-healing assay indicated that wound closure was significantly slowed by NAMPT inhibitors in a dose dependent manner (Supplementary Fig. S7). Similarly, transwell assays showed that migration abilities of NSCLC cells were inhibited by NAMPT inhibitors (Supplementary Fig. S8A). Furthermore, supplement with NMN rescued cell migration abilities as the number of migrating cells significantly increased in the groups with NAMPT inhibitors combined with NMN compared with NAMPT inhibitor groups (Supplementary Fig. S8B). These data demonstrated that NAMPT inhibitors could inhibit NSCLC cell migration.

NAMPT inhibitors inhibit NSCLC proliferation through targeting RAB26

To explore molecular mechanisms of NAMPT inhibitors against NSCLC cells, we next used RNA-seq to investigate FK866-induced alterations of gene expression. The results showed that a total of 1451 genes were upregulated, while 1370 genes were downregulated in FK866-treated H460 cells (Fig. 3A-B). A total of 4801 genes were upregulated, while 1370 genes were downregulated in FK866-treated A549 cells (Fig. 3A-B). The intersecting differentially expressed genes (DEGs) between the H460 and A549 cell lines identified a total of 27 genes that were significantly downregulated ($\log_2$FC≤ -1, P<0.05) (Fig. 3C, Supplementary Table. S4). Among these DEGs, RAB26, a member of Ras superfamilies of small G proteins (RAB family), drew our attention. Recent studies have reported that RAB26 is overexpressed in NSCLC and highly expressed RAB26 is closely related to vesicle-mediated secretion, cell growth, and migration of NSCLC [17–21]. Moreover, high expression of RAB26 correlated with shorter overall survival (OS) (P = 0.02) in patients with NSCLC (Fig. 3D). Therefore, we selected RAB26 for further investigation.

We firstly examined the expression levels of RAB26 mRNA and protein in normal lung cells and NSCLC cells, and the result showed that the expression of RAB26 mRNA and protein in NSCLC cells was higher than normal lung cells (Fig. 3E-F). Further, we examined whether FK866 treatment altered the expression levels of RAB26 mRNA and protein. As expected, FK866 suppressed RAB26 expression in a dose dependent manner in NSCLC cells (Fig. 3G-H).

To clarify whether downregulation of RAB26 mediated the effect of FK866 on NSCLC cells, we next determined the function of RAB26 in NSCLC cells. Two siRNAs were used to interfere with RAB26 expression in H460 and A549 cells, and siRAB26 knockdown significantly inhibited cell viability (Fig. 3I) and DNA synthesis compared with control cells (Fig. 3J). Our results suggested that downregulation of RAB26 recapitulates the inhibitory function of FK866 in NSCLC cells.

Smad3 was shown to mediate the transcription of RAB26 in NSCLC cells [17]. Smad3 is a key protein in the TGF-β1/Smads signaling pathway, and activation of the TGF-β1 signaling promotes metastasis of NSCLC cells [21]. Lv et al. found that there is a negative feedback loop between NAMPT and the TGF-β1 signaling pathway in colorectal cancer cells [22]. However, it is unknown whether NAMPT could regulate RAB26 expression through TGF-β1 signaling. We performed western blot assays to test whether NAMPT inhibitors suppress NSCLC cells via the TGF-β1/Smads axis. As shown in Fig. 4A and Fig. S9, TGF-β1, Smad2, p-Smad2, Smad3, p-Smad3, Smad2/3, Smad4 and RAB26 levels were significantly decreased with NAMPT inhibitors, and consistently, these proteins significantly increased upon supplementation with NMN (Fig. 4B). Collectively, these results suggest that NAMPT inhibitors downregulate RAB26 by inhibiting the TGF-β1/Smads signaling pathway in NSCLC cells.

NAMPT-TGF-β1-Smads-RAB26 axis is activated in human NSCLC and NSCLC BM and predicts poor prognosis

We investigated protein expression of the NAMPT-TGF-β1-Smads-RAB26 axis in patients (10 cases) who underwent surgical resection of primary NSCLC and NSCLC BM (Supplementary Fig. S10). Consistent with our NSCLC cells, NAMPT was highly expressed in NSCLC and NSCLC BM tissues (Fig. 5A). NAMPT, TGF-β1, Smad2, Smad3, Smad4 and RAB26 protein levels were also upregulated in NSCLC and NSCLC BM compared to corresponding peri-tumor tissues (Fig. 5A, Supplementary Fig. S11A and B).

The data from the Kaplan Meier plotter(http://kmplot.com/analysis/) online tool indicated that the OS of NSCLC patients was negatively associated with NAMPT, TGF-β1, Smad2, Smad3 and RAB26 expression (Fig. 5B-F). Thus, patients with high NAMPT-TGF-β1-Smads-RAB26 axis expression had poorer survival.

FK866 combination with cisplatin further prolongs survival in an NSCLC BM model

Cisplatin-based chemotherapy is the first-line treatment for NSCLC [23]. When combined with FK866, cisplatin offers potential for combinatorial chemotherapy for ovarian cancer and cholangiocarcinoma [24, 25]. Moreover,

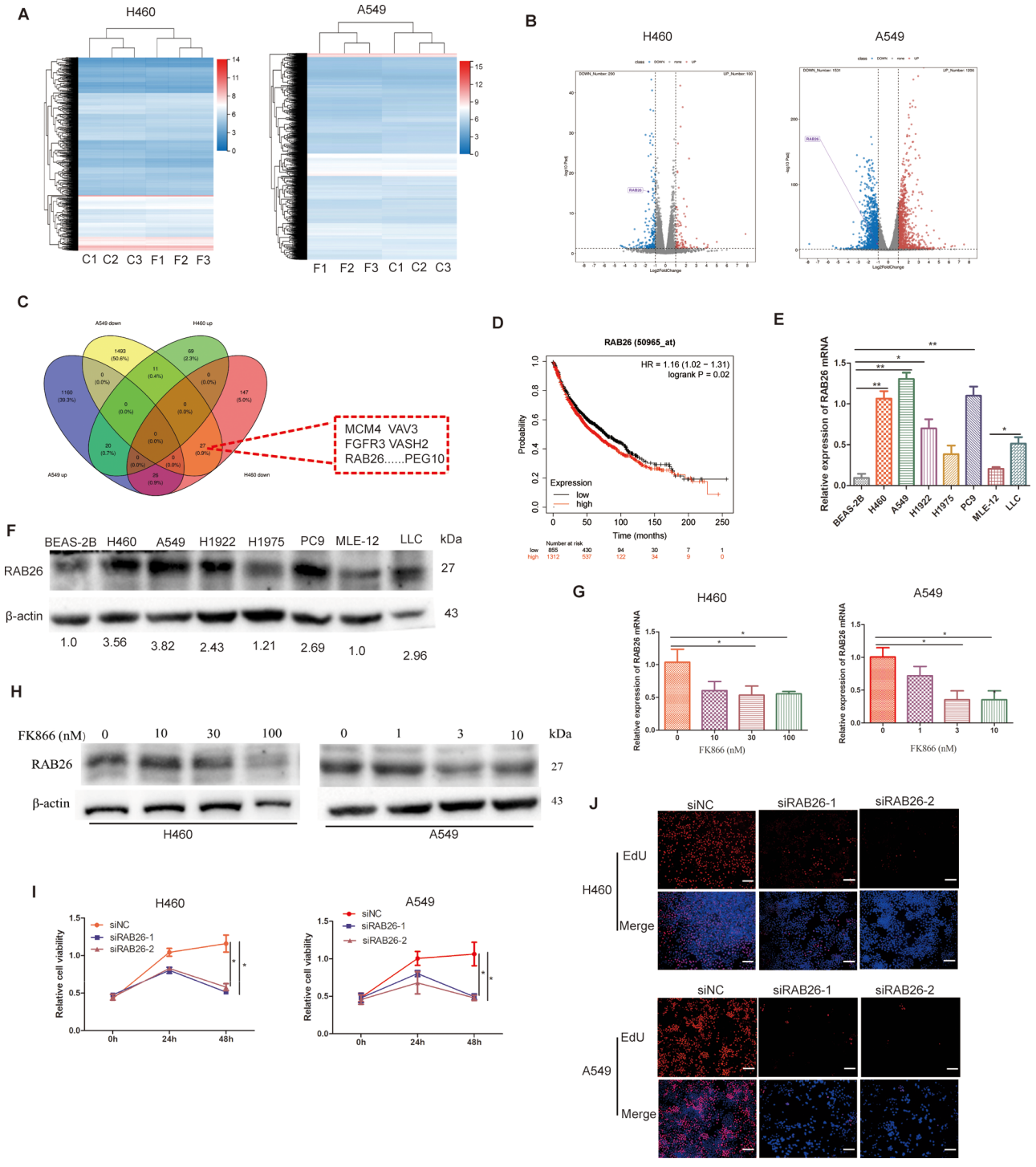

Fig. 3 NAMPT inhibitors inhibit NSCLC proliferation through targeting RAB26. **(A-B)** Heatmap (**A**) and volcano plot (**B**) analyzed using RNA-seq of H460 and A549 cells treated with 0.1% DMSO and FK866 (H460: FK866 30 nmol/L, A549:FK866 3nmol/L) for 48 h. C: 0.1% DMSO, F: FK866. **(C)** The intersection of genes in H460 cells and A549 cells. **(D)** Kaplan-Meier analysis of OS by RAB26 expression data from TCGA. **(E-F)** qPCR (**E**) and western blot (**F**) analyzed RAB26 mRNA and protein expression in normal bronchial epithelial cell lines and NSCLC cell lines, respectively. **(G-H)** qPCR (**G**) and western blot (**H**) analyzed RAB26 mRNA and protein expression in H460 and A549 cells treated with different concentrations of FK866 for 48 h, respectively. **(I-J)** H460 and A549 cells transfected with control siRNA (siNC), RAB26-siRNA1 (siRAB26-1), and RAB26-siRNA2 (siRAB26-2) were used to analyze cell viability by CCK8 (**I**), and DNA synthesis by EdU assay (**J**) (*Scale bar*: 150 μm). β-actin was used as loading control for western blot. **P*<0.05, ** *P* < 0.01, *** *P* < 0.001

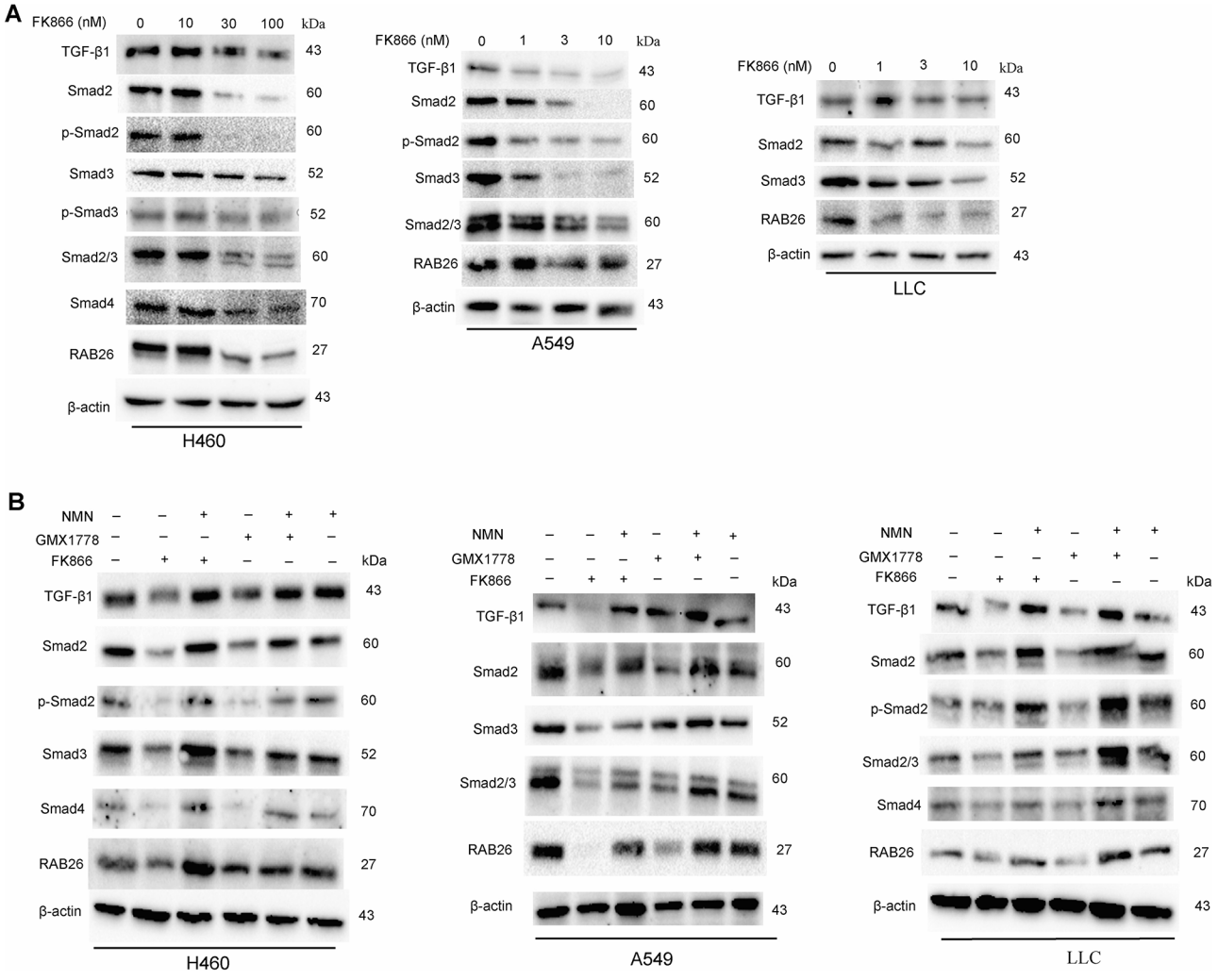

Fig. 4 NAMPT inhibitors inhibit the TGF-β1/Smads/RAB26 axis in NSCLC cells. **(A)** Western blot analysis of TGF-β1/Smads/RAB26 axis key proteins in H460, A549 and LLC cells treated with different concentrations of FK866 for 48 h. **(B)** Impact of supplementation with 1mmol/L NMN on TGF-β1/Smads/RAB26 axis key protein expression in H460, A549 and LLC cells by western blot assay. (H460: FK866 30nmol/L, GMX1778 30nmol/L; A549: FK866 3nmol/L, GMX1778 20nmol/L; LLC: FK866 3nmol/L, GMX1778 15 nmol/L) β-actin was used as loading control

knocking down RAB26 (siRNA) improved NSCLC sensitivity to cisplatin as the combined therapy of siRAB26 knockdown with cisplatin improved antitumor efficacy compared with monotherapies in vitro [20]. We thus investigated the therapeutic potential of FK866 combined with cisplatin in the NSCLC BM mouse model of LLC-Luc (Fig. 6A). In this model, cisplatin alone had no beneficial effect (Fig. 6B-D). The group of combination of FK866 with cisplatin showed statistically significant responses in terms of tumor volume, body weight and survival analysis compared with the FK866 group or the cisplatin group (Fig. 6B-D). Median survival of cisplatin alone-treated and FK866 alone-treated mice was only 19 days and 38 days, respectively, as compared with 46 days with the combination therapy ($P < 0.01$) (Fig. 6D).

Discussion

To date, NSCLC BM is a common disease with a dismal outcome. This is partly explained by NSCLC resistance to molecular targeted therapy and inability of systemic chemotherapy to cross the BBB. Therefore, it is necessary to develop innovative therapy for NSCLC BM. In this study, we show that FK866 could inhibit intracranial tumor growth in a NSCLC BM model, increasing the survival of animals. Specifically, we confirmed: (1) NAMPT is upregulated in NSCLC BM and NSCLC tissues; (2) FK866 and GMX1778, two small molecule NAMPT inhibitors, deplete NAD^+ pool in NSCLC cells; (3) NAMPT inhibitors suppress NSCLC cells proliferation, colony formation, and migration, and induce cell apoptosis; (4) Supplementation with NAD^+ precursor NMN rescued the effects of NAMPT inhibitors on NSCLC cells. For further mechanistic understanding, we revealed RAB26

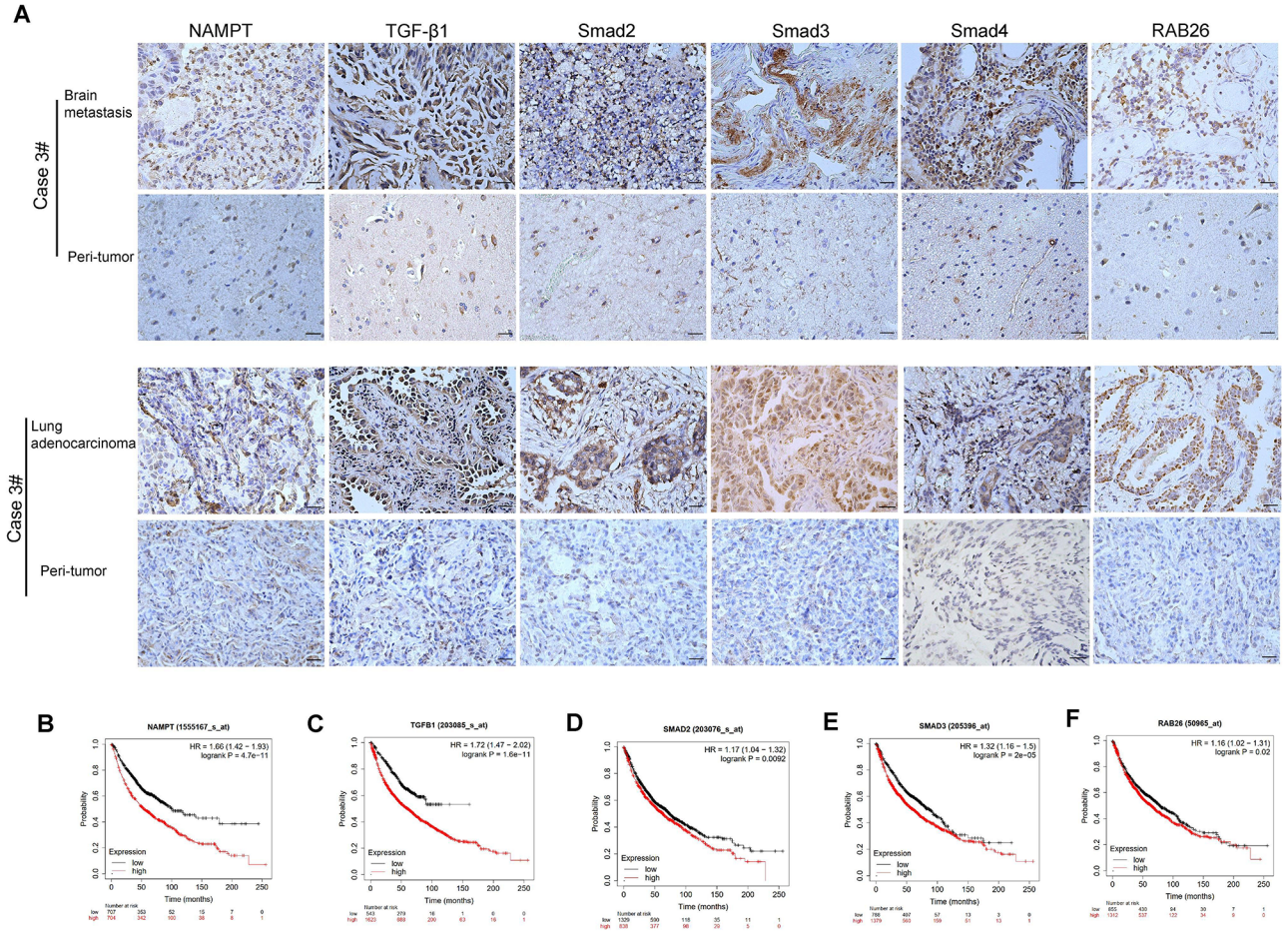

Fig. 5 NAMPT-TGF-β1-Smads-RAB26 axis is activated in human NSCLC and NSCLC BM and predicts poor prognosis. **(A)** NAMPT, TGF-β1, Smad2, Smad3, Smad4 and RAB26 expression in NSCLC and NSCLC BM tissues and corresponding peri-tumor tissues. (*Scale bar*: 150 μm). **(B-F)** Kaplan-Meier analysis of OS by NAMPT (**B**), TGF-β1 (**C**), Smad2 (**D**), Smad3 (**E**), and RAB26 (**F**) expression data from NSCLC TCGA

as a novel downstream target of NAMPT inhibitors in NSCLC, and disruption of NAMPT-mediated NAD^+ metabolism suppressed the TGF-β1/smads/RAB26 axis, inhibiting NSCLC cells proliferation (Fig. 6E).

NAD^+ is an important cofactor in oxidation reduction reactions and involved in various energy processes in the body, including fatty acids, glycolysis, and serine biosynthesis [6, 8]. In addition, NAD^+ is a substrate for the reactions catalyzed by SIRT, PARPs and cADPRs. High levels NAD^+ are involved in non-redox processes such as DNA repair, translation modification, aging, inflammation, cell signal transduction, and apoptosis [26]. Since sustaining proliferative signaling is a hallmark of tumor cells [27], NAD^+ is needed to support their proliferation [28]. In mammals, tryptophan, nicotinamide (Nam) and nicotinic acid (NA) are the main precursors of NAD^+ biosynthesis, of which Nam is the most important in the synthesis of NAD^+ [29]. NAMPT, the rate-limiting enzyme in NAD^+ synthesis from Nam, is overexpressed in multiple tumors and a promising treatment target in tumors [10–12]. In this study, we identified that NAMPT is up-regulated in NSCLC BM tissues and NAMPT inhibitors could inhibit intracranial tumor growth in NSCLC BM, increasing animal survival. These results support further exploration of NAMPT inhibitors as new therapeutics in NSCLC BM patients.

We comprehensively characterized the effects of NAMPT inhibitors in NSCLC cells. Firstly, we show that NAMPT inhibitors inhibit NSCLC cell viability in a dose-dependent manner. We provide experimental evidence that NAMPT inhibitors inhibit NSCLC cell proliferation, colony formation, and migration, and induce cell apoptosis. Moreover, supplementation of NAD^+ precursor NMN could rescue the effects of NAMPT inhibitors on NSCLC cells. Tumor cell growth is the direct result of imbalance between cell gain and cell loss, where the rate of cell proliferation exceeds the rate of apoptosis [30]. NAMPT inhibitors decreased the NAD^+ pool in cancer cells, thus inhibiting ATP synthesis, which could cause a decrease in cell proliferation and an increase in cell apoptosis [31, 32]. However, the mechanisms of NAMPT inhibitors inhibiting proliferation and inducing apoptosis

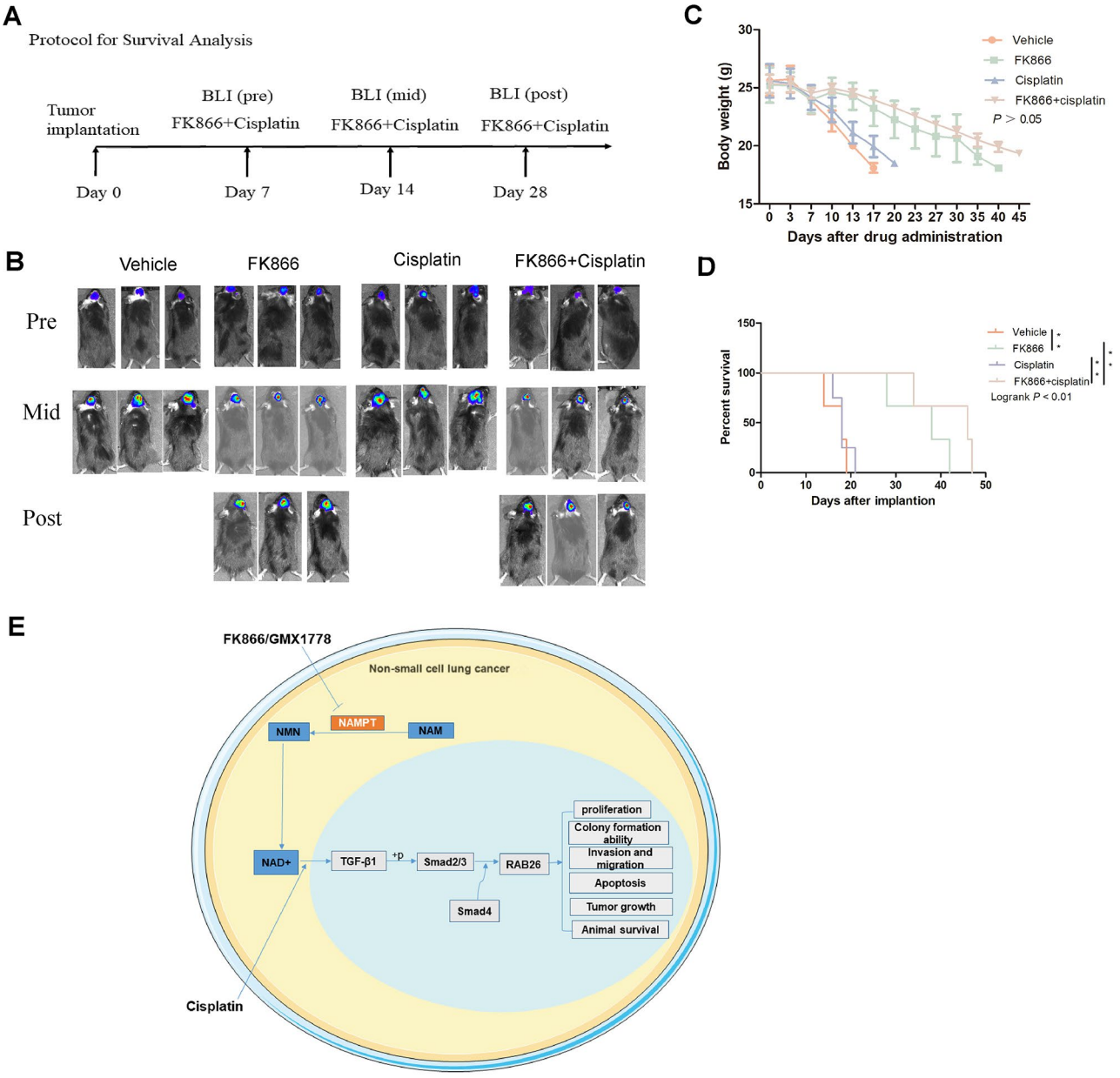

Fig. 6 FK866 combines with cisplatin to inhibit NSCLC BM tumor growth and increase animal survival. **(A-B)** LLC-luc-bearing mice were treated with vehicle, FK866, cisplatin, FK866 combined with cisplatin beginning on 7 days after tumor implantation. BLI was performed on days 7, 14, and 28 while on treatment. **(C)** Mouse weight was recorded for each group. **(D)** Survival data were collected for each group and analyzed by Kaplan–Meier analysis. ** $P < 0.01$. (**E**) Graphic abstract of the current work

is poorly defined. In this study, our transcriptome analysis revealed that various genes affected by FK866 were functionally associated with multiple pathways. Specifically, we identified RAB26 as a target gene linked to FK866 cytotoxicity in NSCLC cells.

RAB26 impacts cell survival and stress responses [33] and is closely associated with lung disease [34–36]. For example, RAB26 deficiency aggravates lipopolysaccharide-induced lung tissue injury [34]. The survival time of RAB26 knock-down mice was decreased compared with wildtype mice [35]. In addition, RAB26 was decreased in the lung tissue of COPD patients, and restoring RAB26 in the airway epithelium is a potential strategy for treating airway inflammation and COPD [36]. It should be noted that RAB26 is identified as a tumor promoter and loss of RAB26 inhibited the growth of NSCLC [17–21]. Consistent with the previous studies, our study showed that RAB26 mRNA and protein in NSCLC cells were significantly higher than normal lung cells, and knocking down RAB26 significantly inhibited cell viability and

DNA synthesis compared with control cells. In addition, FK866 inhibited RAB26 expression in NSCLC cells in a dose dependent manner, suggesting oncogenic RAB26 as a downstream target. NAMPT inhibitors regulate cell proliferation, at least in part, via targeting RAB26 in NSCLC cells.

SMAD3 is an up-stream regulator of RAB26 [17]. Smad3 is a key protein in the TGF-β1/Smads signaling pathway, and activation of the TGF-β1 signaling promotes metastasis of NSCLC cells [21]. In addition, there is a negative feedback loop between NAMPT and the TGF-β1 signaling pathway in colorectal cancer cells [22]. We explored whether NAMPT inhibitors inhibited the TGF-β1/Smads/RAB26 axis. We showed that NAMPT inhibitors significantly decreased the key proteins of TGF-β1/Smads and RAB26, and NMN rescued expression of these proteins. In this context, we reason that inhibition of the TGF-β1/Smads/RAB26 axis represents a key molecular mechanism of therapeutic NAD^+ metabolism disruption in NSCLC cells.

Cisplatin has been widely used for treatment of numerous human cancers, including bladder, head and neck, lung, ovarian, and testicular cancers [23]. FK866 combined with cisplatin offers potential for combinatorial chemotherapy for ovarian cancer and cholangiocarcinoma [23, 24]. However, substantial limitations exist in use of cisplatin for NSCLC BM due to difficulties in penetration across the BBB. To improve utilization, cisplatin is commonly used in combination with other drugs for treating brain cancer. For example, Zou et al. demonstrated that temozolomide and cisplatin had promising potential for GBM therapy [37]. FK866 induces apoptosis by depleting cellular NAD^+ levels and could cross the BBB. However, Phase I clinical studies showed that FK866 had dose-dependent toxicities in humans (38, 39), including suppression of the bone marrow, gastrointestinal toxicities, retinal toxicity, along with limited antitumor efficacy and poor pharmacokinetics. In this study, we used FK866 combined with cisplatin in NSCLC BM, and showed that the combination significantly prolonged the survival of animals, compared with the FK866 or cisplatin monotherapy group. These results suggest that targeting NAD^+ using clinically applicable NAMPT inhibitors, such as FK866, in conjunction with cisplatin represents a promising therapeutic strategy in NSCLC BM and may allow dose reduction in NAMPT inhibitors to mitigate their toxicity issues.

Our study has some limitations. Firstly, we used intracranial implantation of LLC cells as an in vivo BM model, which is not a "brain seeking" model representing the clinical scenario of BM. Serial intracardiac implantation of fluorescently labeled LLC cells followed by flow-cytometric sorting of micro BM can enrich brain-seeking cells and help establish a new BM model. Secondly, the number of primary tumor and paired NSCLC BM was only 10 pairs, and validation with increased sample size will be needed in future research.

In summary, this study identified the critical role of NAD^+ metabolism in NSCLC BM. NAMPT inhibition decreased intracranial tumor growth and prolonged animal survival, which was enhanced by combination with cisplatin. Targeting NAD^+ metabolism inhibited the proliferation and migration of NSCLC cells by inhibiting the TGF-β1/Smads/RAB26 axis. Taken together, our findings provide new therapeutic strategies for NSCLC BM, which may benefit patients with NSCLC BM.

Abbreviations

NAD	Nicotinamide adenine dinucleotide
NSCLC BM	Non-small cell lung cancer with brain metastasis
NAMPT	Nicotinamide phosphoribosyl transferase
BiR	BRAF inhibitor resistant
LLC-luc	luciferase expression
IHC	Immunohistochemistry
DMSO	Dimethyl sulfoxide
CCK8	Cell Counting Kit-8

Supplementary Information

The online version contains supplementary material available at https://doi.org/10.1186/s40478-025-01967-4.

Supplementary Material 1: Figure S1. NAMPT inhibitors inhibit NSCLC subcutaneous tumor growth. (A-C) C57BL/6J mice ($n = 5$–8 mice per group) were injected subcutaneously with LLC cells. LLC-bearing mice were treated with vehicle, FK866, GMX1778 on tumor implation day 7. On day 14, the mice were pictured (A), then tumors were removed (B) and weighed (C). *$P<0.05$, ** $P<0.01$. Figure S2. NAMPT inhibitors inhibit NSCLC cell viability. (A-B) H460, A549 and LLC cells were treated with 0.1% DMSO, FK866 and GMX1778 for 72 h, and then cell viability measured by CCK-8 assay. Figure S3. NAMPT inhibitors inhibit DNA synthesis in NSCLC cells. (A) H460, A549 and LLC cells treated with different concentrations of FK866 and GMX1778 for 48 h were tested for DNA synthesis by EdU assay. (B) The impact of supplementation with 1mmol/L NMN for 48 h on DNA synthesis examined by EdU assay. (H460: FK866 30nmol/L, GMX1778 30nmol/L; A549: FK866 3nmol/L, GMX1778 20nmol/L; LLC: FK866 3nmol/L, GMX1778 15 nmol/L) (***Scale bar***: 200 μm). Figure S4. NAMPT inhibitors inhibit colony formation by NSCLC cells. (A) H460, A549 and LLC cells treated with different concentrations of FK866 and GMX1778 were assayed for colony formation. (B and C) Impact of supplementation with 1mmol/L NMN for 12 days on colony formation was measured. (H460: FK866 30nmol/L, GMX1778 30nmol/L; A549: FK866 3nmol/L, GMX1778 20nmol/L; LLC: FK866 3nmol/L, GMX1778 15 nmol/L) *$P<0.05$, ** $P<0.01$, ***, $P<0.001$. Figure S5. NAMPT inhibitors induce apoptosis and arrest cell cycle. (A) Flow cytometry analysis of H460, A549 and LLC cells apoptosis treated with different concentrations of FK866 and GMX1778 for 48 h. Quantification of the total proportion of Annexin V-positive (early apoptotic) cells and 7ADD-stained double positive (late apoptotic) cells. (B) Western blot analysis of cell apoptosis proteins in H460, A549 and LLC cells treated with different concentrations of FK866 for 48 h. (C) Western blot analysis of cell apoptosis proteins in H460 and LLC cells treated with different concentrations of GMX1778 for 48 h. (D) Flow cytometry analysis of H460, A549 and LLC cells treated with different concentrations of FK866 for 48 h. Quantification of the cell cycle profile. (E-F) Western blot analysis of cell cycle proteins in H460 and LLC cells treated with different concentrations of FK866 (E) and GMX1778 (F) for 48 h. (G) Cell apoptosis proteins and cell cycle proteins were measured by western blot with and without supplementation with 1mmol NMN for 48 h. (H460: FK866 30nmol/L, GMX1778 30nmol/L; A549: FK866 3nmol/L, GMX1778 20nmol/L; LLC: FK866 3nmol/L, GMX1778 15 nmol/L) β-actin was used as loading control for western blot. *$P<0.05$, ** $P<0.01$, ***, $P<0.001$. Figure S6. NAMPT inhibitors induce

apoptosis in A549 cells. (A) NAMPT inhibitor-induced (3 nmol/L FK866, 20nmol/L GMX1778) apoptosis was measured by flow cytometry with and without supplementation with 1mmol NMN for 48 h. (B) Quantification of the total proportion of cell apoptosis. ** $P < 0.01$. Figure S7. NAMPT inhibitors reduce migration of NSCLC cells. (A-B) H460, A549 and LLC cells were treated with different concentrations of FK866 for 48 h. Cell migration was measured by wound-healing assays. (C-D) H460 and LLC cells were treated with different concentrations of GMX1778 for 48 h. Cell migration was measured by wound-healing assays. *$P<0.05$, ** $P < 0.01$, ***, $P < 0.001$. Figure S8. NAMPT inhibitors reduce transwell migration of NSCLC cells. (A) H460, A549 and LLC cells were treated with different concentrations of FK866 and GMX1778 for 48 h. Cell migration was measured by transwell assays. (B) Cell migration was measured by transwell assays with and without supplementation with 1mmol/L NMN for 48 h.(H460: FK866 30nmol/L, GMX1778 30nmol/L; A549: FK866 3nmol/L, GMX1778 20nmol/L; LLC: FK866 3nmol/L, GMX1778 15 nmol/L) ** $P < 0.01$, ***, $P < 0.001$. Figure S9. NAMPT inhibitors downregulate TGF-β1/Smads/RAB26 signaling axis proteins in NSCLC cells. Western blot analysis of TGF-β1/Smads/RAB26 axis key protein expression in H460 and A549 cells treated with different concentrations of GMX1778 for 48 h. β-actin was used as loading control. Figure S10. A patient who underwent surgical resection for primary NSCLC and NSCLC BM. Hematoxylin and eosin staining of tumor tissues (A, BM and B, primary) and the corresponding peri-tumor tissues. (***Scale bar***: 150 μm), Figure S11. NAMPT-TGF-β1-smads-RAB26 axis protein expression in 2 cases of primary NSCLC and NSCLC BM. Immunohistochemistry for the indicated proteins is presented. (***Scale bar***: 150 μm). Supplementary Table S1. Primary antibodies used in the study. Supplementary Table S2. qRT-PCR primer information in the study. Supplementary Table S3. Target sequences of siRNAs in the study. Supplementary Table S4. The intersection of genes in H460 cell and A549 cell genes with a fold change ≥ 2 or ≤ -2 and P value ≤ 0.005.

Acknowledgements
The authors thank Dr. Shuangyin Han (Faculty of Henan Provincial People's Hospital, Zhengzhou University) for his help in critical reading of the manuscript and helpful discussion.

Author contributions
All authors contributed to the study conception and design. Material preparation, data collection and first draft of the manuscript were written by Liyun Zhou, Zhiying Li and Shengli Zhou; Material preparation and data analysis were performed by Bin Wang, Zhen Liang, Hang Zhang, Lin Duan, Dongxu Zhao, Hang Ren and Luyao Cheng; The Project administration and manuscript edit were by Hiroaki Wakimoto and Ming Li. And all authors commented on previous versions of the manuscript. All authors read and approved the final manuscript.

Funding
This work was supported by 23456 Project of Henan Provincial People's Hospital (ZC20200349).

Data availability
The datasets generated during and/or analysed during the current study are available from the corresponding author on reasonable request.

Declarations

Ethics and approval and consent to participate
This study was approved by the Ethics Committee of Zhengzhou University People's Hospital, Henan province, China (Approval No.H2023-07-025). The ethics committee of Zhengzhou University People's Hospital waived the need for informed consent due to the retrospective nature of the study. All procedures were conducted by following the Declaration of Helsinki. All methods were carried out in accordance with relevant guidelines and regulations in the declaration.

Conflict of interest
There are no potential conflicts of interest to be disclosed.

Author details
[1]Department of Neurosurgery, Henan Provincial People's Hospital, People's Hospital of Zhengzhou University, People's Hospital of Henan University, Zhengzhou 450003, People's Republic of China
[2]Department of Neurosurgery, The 7th People's Hospital of Zhengzhou, Zhengzhou 450000, China
[3]Department of Pathology, Henan Provincial People's Hospital, People's Hospital of Zhengzhou University, People's Hospital of Henan University, Zhengzhou 450003, People's Republic of China
[4]Department of Neurosurgery, The Affiliated Cancer Hospital of Zhengzhou University & Henan Cancer Hospital, Zhengzhou 450008, China
[5]Department of Neurosurgery, Massachusetts General Hospital, Harvard Medical School, Boston, MA 02114, USA

Received: 14 July 2024 / Accepted: 18 February 2025
Published online: 11 March 2025

References

1. Siegel RL, Miller KD, Wagle NS, Jemal A (2023) Cancer statistics, 2023. CA Cancer J Clin 73:17–48. https://doi.org/10.3322/caac.21763
2. Siegel RL, Miller KD, Fuchs HE, Jemal A (2022) Cancer statistics, 2022. CA Cancer J Clin 72:7–33. https://doi.org/10.3322/caac.21708
3. Langley RR, Fidler IJ (2011) The seed and soil hypothesis revisited–the role of tumor-stroma interactions in metastasis to different organs. Int J Cancer 128:2527–2535. https://doi.org/10.1002/ijc.26031
4. Olmez I, Donahue BR, Butler JS, Huang Y, Rubin P, Xu Y (2010) Clinical outcomes in extracranial tumor sites and unusual toxicities with concurrent whole brain radiation (WBRT) and erlotinib treatment in patients with non-small cell lung cancer (NSCLC) with brain metastasis. Lung Cancer 70:174–179. https://doi.org/10.1016/j.lungcan.2010.01.018
5. Preusser M, Capper D, Ilhan-Mutlu A, Berghoff AS, Birner P, Bartsch R et al (2012) Brain metastases: pathobiology and emerging targeted therapies. Acta Neuropathol 123:205–222. https://doi.org/10.1007/s00401-011-0933-9
6. Navas LE, Carnero A (2022) Nicotinamide adenine dinucleotide (NAD) metabolism as a relevant target in Cancer. Cells 11:2627. https://doi.org/10.3390/cells11172627
7. Xie N, Zhang L, Gao W, Huang C, Huber PE, Zhou X et al (2020) NAD + metabolism: pathophysiologic mechanisms and therapeutic potential. Signal Transduct Target Ther 5:227. https://doi.org/10.1038/s41392-020-00311-7
8. Liu Y, Sun Y, Guo Y, Shi X, Chen X, Feng W et al (2023) An overview: the diversified role of mitochondria in Cancer metabolism. Int J Biol Sci 19:897–915. https://doi.org/10.7150/ijbs.81609
9. Moreira JD, Hamraz M, Abolhassani M, Bigan E, Pérès S, Paulevé L et al (2016) The redox status of Cancer cells supports mechanisms behind the Warburg effect. Metabolites 6:33. https://doi.org/10.3390/metabo6040033
10. Touat M, Sourisseau T, Dorvault N, Chabanon RM, Garrido M, Morel D et al (2018) DNA repair deficiency sensitizes lung cancer cells to NAD + biosynthesis Blockade. J Clin Invest 128:1671–1687. https://doi.org/10.1172/JCI90277
11. Navas LE, Blanco-Alcaina E, Suarez-Martinez E, Verdugo-Sivianes EM, Espinosa-Sanchez A, Sanchez-Diaz L et al (2023) NAD pool as an antitumor target against cancer stem cells in head and neck cancer. J Exp Clin Cancer Res 42:55. https://doi.org/10.1186/s13046-023-02631-2
12. Wu J (2022) Targeting nicotinamide adenosine dinucleotide (NAD) in diffuse gliomas. Neuro Oncol 24:245–246. https://doi.org/10.1093/neuonc/noab265
13. Li M, Kirtane AR, Kiyokawa J, Nagashima H, Lopes A, Tirmizi ZA et al (2020) Local targeting of NAD + Salvage pathway alters the immune tumor microenvironment and enhances checkpoint immunotherapy in glioblastoma. Cancer Res 80:5024–5034. https://doi.org/10.1158/0008-5472.CAN-20-1094
14. Tateishi K, Wakimoto H, Iafrate AJ, Tanaka S, Loebel F, Lelic N et al (2015) Extreme vulnerability of IDH1 mutant cancers to NAD + Depletion. Cancer Cell 28:773–784. https://doi.org/10.1016/j.ccell.2015.11.006
15. Audrito V, Managò A, La Vecchia S, Zamporlini F, Vitale N, Baroni G et al (2018) Nicotinamide phosphoribosyltransferase (NAMPT) as a therapeutic target in BRAF-Mutated metastatic melanoma. J Natl Cancer Inst 110. https://doi.org/10.1093/jnci/djx198
16. Kiyokawa J, Kawamura Y, Ghouse SM, Acar S, Barçın E, Martínez-Quintanilla J et al (2021) Modification of extracellular matrix enhances oncolytic adenovirus immunotherapy in glioblastoma. Clin Cancer Res 27:889–902. https://doi.org/10.1158/1078-0432.CCR-20-2400

17. Ren H, Yang B, Li M, Lu C, Li X (2022) RAB26 contributes to the progression of non-small cell lung cancer after being transcriptionally activated by SMAD3. Bioengineered 13:8064–8075. https://doi.org/10.1080/21655979.2022.2051853
18. Liu Q, Wang D, Xu Z, Huang C, Zhang C, He B et al (2019) Targeted delivery of Rab26 SiRNA with precisely tailored DNA Prism for lung Cancer therapy. ChemBioChem 20(9):1139–1144. https://doi.org/10.1002/cbic.201800761
19. Yang XY, Liao JJ, Xue WR (2019) FMNL1 down-regulation suppresses bone metastasis through reducing TGF-β1 expression in non-small cell lung cancer (NSCLC). Biomed Pharmacother 117:109126. https://doi.org/10.1016/j.biopha.2019.109126
20. Wang B, Zhang R, Wang Y, Qian H, Wu D, He B et al (2023) Targeting Rab26 to conquer Cisplatin-Resistant lung Cancer with Self-Assembled DNA nanomaterials. Biomacromolecules 24:2063–2074. https://doi.org/10.1021/acs.biomac.2c01493
21. Huang Y, Chen Z, Lu T, Bi G, Li M, Liang J et al (2021) HIF-1α switches the functionality of TGF-β signaling via changing the partners of Smads to drive glucose metabolic reprogramming in non-small cell lung cancer. J Exp Clin Cancer Res 40:398. https://doi.org/10.1186/s13046-021-02188-y
22. Lv X, Zhang J, Zhang J, Guan W, Ren W, Liu Y et al (2021) A negative feedback loop between NAMPT and TGF-β signaling pathway in colorectal Cancer cells. Onco Targets Ther 14:187–198. https://doi.org/10.2147/OTT.S282367
23. Dasari S, Tchounwou PB (2014) Cisplatin in cancer therapy: molecular mechanisms of action. Eur J Pharmacol 740:364–378. https://doi.org/10.1016/j.ejphar.2014.07.025
24. Nacarelli T, Fukumoto T, Zundell JA, Fatkhutdinov N, Jean S, Cadungog MG et al (2020) NAMPT Inhibition suppresses Cancer Stem-like cells associated with Therapy-Induced senescence in ovarian Cancer. Cancer Res 80(4):890–900. https://doi.org/10.1158/0008-5472.CAN-19-2830
25. Pant K, Richard S, Peixoto E, Yin J, Seelig DM, Carotenuto P et al (2023) The NAMPT inhibitor FK866 in combination with cisplatin reduces cholangiocarcinoma cells growth. Cells 12:775. https://doi.org/10.3390/cells12050775
26. Navas LE, Carnero A (2021) NAD + metabolism, stemness, the immune response, and cancer. Signal Transduct Target Ther 6:2. https://doi.org/10.1038/s41392-020-00354-w
27. Hanahan D, Weinberg RA (2011) Hallmarks of cancer: the next generation. Cell 144(5):646–674. https://doi.org/10.1016/j.cell.2011.02.013
28. Khan JA, Forouhar F, Tao X, Tong L (2007) Nicotinamide adenine dinucleotide metabolism as an attractive target for drug discovery. Expert Opin Ther Targets 11:695–705
29. Campbell JM (2022) Supplementation with NAD + and its precursors to prevent cognitive decline across disease contexts. Nutrients 14:3231. https://doi.org/10.3390/nu14153231
30. Morana O, Wood W, Gregory CD (2022) The apoptosis paradox in Cancer. Int J Mol Sci 23:1328. https://doi.org/10.3390/ijms23031328
31. Conforti I, Benzi A, Caffa I, Bruzzone S, Nencioni A, Marra A (2023) Iminosugar-Based nicotinamide phosphoribosyltransferase (NAMPT) inhibitors as potential Anti-Pancreatic Cancer agents. Pharmaceutics 15:1472. https://doi.org/10.3390/pharmaceutics15051472
32. Ghanem MS, Caffa I, Monacelli F, Nencioni A (2024) Inhibitors of NAD + Production in Cancer treatment: state of the Art and perspectives. Int J Mol Sci 25:2092. https://doi.org/10.3390/ijms25042092
33. Chen H, Yuan M, Huang C, Xu Z, Li M, Zhang C et al (2019) Endothelial cell inflammation and barriers are regulated by the Rab26-Mediated balance between β2-AR and TLR4 in pulmonary microvessel endothelial cells. Mediators Inflamm 2019:7538071. https://doi.org/10.1155/2019/7538071
34. Dong W, He B, Qian H, Liu Q, Wang D, Li J et al (2018) RAB26-dependent autophagy protects adherens junctional integrity in acute lung injury. Autophagy 14:1677–1692. https://doi.org/10.1080/15548627.2018.1476811
35. Zhang W, Wang Y, Li C, Xu Y, Wang X, Wu D et al (2021) Extracellular CIRP-Impaired Rab26 restrains EPOR-Mediated macrophage polarization in acute lung injury. Front Immunol 12:768435. https://doi.org/10.3389/fimmu.2021.768435
36. He BF, Wu YX, Hu WP, Hua JL, Han Y, Zhang J (2023) ROS induced the Rab26 promoter hypermethylation to promote cigarette smoking-induced airway epithelial inflammation of COPD through activation of MAPK signaling. Free Radic Biol Med 195:359–370. https://doi.org/10.1016/j.freeradbiomed.2023.01.001
37. Zou Y, Wang Y, Xu S, Liu Y, Yin J, Lovejoy DB et al (2022) Brain Co-Delivery of Temozolomide and cisplatin for combinatorial glioblastoma chemotherapy. Adv Mater 34:e2203958. https://doi.org/10.1002/adma.202203958
38. von Heideman A, Berglund A, Larsson R, Nygren P (2010) Safety and efficacy of NAD depleting cancer drugs: results of a phase I clinical trial of CHS 828 and overview of published data. Cancer Chemother Pharmacol 65:1165–1172. https://doi.org/10.1007/s00280-009-1125-3
39. Holen K, Saltz LB, Hollywood E, Burk K, Hanauske AR (2008) The pharmacokinetics, toxicities, and biologic effects of FK866, a nicotinamide adenine dinucleotide biosynthesis inhibitor. Invest New Drugs 26:45–51. https://doi.org/10.1007/s10637-007-9083-2

Publisher's note